$^{40}Ar/^{39}Ar$ Geochronology Results for the Chriss Canyon, Hells Kitchen Canyon SW, Jordan Narrows, Lehi, Mussentuchit Flat, Springdale West, and Veyo Quadrangles, Utah

by

Utah Geological Survey and
New Mexico Geochronology Research Laboratory

Bibliographic citation for this data report:

Utah Geological Survey and New Mexico Geochronology Research Laboratory, 2007, $^{40}Ar/^{39}Ar$ Geochronology Results for the Chriss Canyon, Hells Kitchen Canyon SW, Jordan Narrows, Lehi, Mussentuchit Flat, Springdale West, and Veyo quadrangles, Utah: Utah Geological Survey Open-File Report 495, variously paginated, also available online, <http://geology.utah.gov/online/ofr/ofr-495.pdf>.

OPEN-FILE REPORT 495
UTAH GEOLOGICAL SURVEY
a division of
Utah Department of Natural Resources
2007

Introduction

This Open-File Report makes available raw analytical data from laboratory procedures completed to determine the age of rock samples collected during geologic mapping funded or partially supported by the Utah Geological Survey (UGS). The references listed in table 1 report the age of the samples and generally provide additional information such as the sample location, geologic setting, and significance or interpretation of the samples in the context of the area in which they were collected. This report was prepared by the New Mexico Geochronology Research Laboratory (NMRGL) under contract to the UGS. These data are highly technical in nature and proper interpretation requires considerable training in the applicable geochronologic techniques.

Table 1. Sample numbers and locations.

Sample #	7.5' quadrangle	Latitude	Longitude	Reference
ZP 1501	Springdale West	37° 12' 41.8"	113° 06' 20.5"	Willis and others (in prep.)
VY111902-7	Veyo	37° 16' 29.4"	113° 42' 17.5"	Hayden (in prep.)
MW1	Mussentuchit Flat	38° 41' 10"	111° 13' 43"	Doelling (2004)
HM1	Mussentuchit Flat	38° 41' 34"	111° 07' 35"	Doelling (2004)
PR-15	Chriss Canyon	39° 29' 05"	111° 52' 04"	Felger and others (in prep.)
JN22703-1	Jordan Narrows	40° 23' 43.4"	111° 59' 37.1"	Biek (2005a)
PR-9	Hells Kitchen Canyon SW	39° 21' 27"	111° 56' 57"	Felger and others (in prep.)
L33103-9	Lehi	40° 27' 59.4"	111° 50' 28.5"	Biek (2005b)

Location data based on NAD27.

Disclaimer

This Open-File release is intended as a data repository for technical analytical information gathered in support of various geologic mapping projects. The data are presented as received from the NMGRL and do not necessarily conform to UGS technical or editorial standards. Therefore, it may be premature for an individual or group to take actions based on the contents of this report.

The Utah Department of Natural Resources, Utah Geological Survey, makes no warranty, expressed or implied, regarding the suitability of this product for a particular use. The Utah Department of Natural Resources, Utah Geological Survey, shall not be liable under any circumstances for any direct, indirect, special, incidental, or consequential damages with respect to claims by users of this product.

References to geologic reports that cite or explain samples analyzed in this report

Biek, R.F., 2005a, Geologic map of the Jordan Narrows quadrangle, Salt Lake and Utah Counties, Utah: Utah Geological Survey Map 208, 2 plates, scale 1:24,000.

Biek, R.F., 2005b, Geologic map of the Lehi quadrangle and part of the Timpanogos Cave quadrangle, Salt Lake and Utah Counties, Utah: Utah Geological Survey Map 210, 2 plates, scale 1:24,000.

Doelling, H.H., 2004, Interim geologic map of the east half of the Salina 30' x 60' quadrangle, Emery, Sevier, and Wayne Counties, Utah: Utah Geological Survey Open-File Report 438, scale 1:62,500.

Felger, T.J., Clark, D.L., and Hylland, M.D., 2007, Geologic map of the Skinner Peaks quadrangle, Juab and Sanpete Counties, Utah: Utah Geological Survey Map 223, scale 1:24,000.

Hayden, J.M., in preparation, Geologic map of the Veyo quadrangle, Washington County, Utah: Utah Geological Survey Map, scale 1:24,000.

Willis, G.C., Doelling, H.H., Solomon, B.J., and Sable, E.G., in preparation, Geologic map of the Springdale West quadrangle, Washington County, Utah: Utah Geological Survey Map, scale 1:24,000.

$^{40}Ar/^{39}Ar$ Geochronology Results

By

Lisa Peters

SEPTEMBER 30, 2003

Prepared for

Robert Biek
Utah Geological Survey
1594 West North Temple, Suite 3110
PO Box 146100
Salt Lake City, Utah 84114-6100

NEW MEXICO GEOCHRONOLOGY RESEARCH LABORATORY (NMGRL)

CO-DIRECTORS

DR. MATTHEW T. HEIZLER

DR. WILLIAM C. MCINTOSH

LABORATORY TECHNICIANS

LISA PETERS

RICHARD P. ESSER

Internal Report #: NMGRL-IR-372

Introduction

This report presents $^{40}Ar/^{39}Ar$ dating results from a set of eight samples submitted for dating by Robert Biek of the Utah Geological Survey. Samples are listed in Table 1, together with field identifications of sampled units where available.

Table 1. Brief summary of results.

Sample	Phase	Unit	Age±2σ (Ma)	Comments
ZP 1501	groundmass concentrate	Crater Hill basalt	0.10±0.08	very low precision
VY111902-7	groundmass concentrate	Veyo basalt	0.69±0.04	well-behaved age spectrum
MW1	biotite	Sill from San Rafael Swell	4.35±0.04	well-behaved age spectrum
HM1	biotite	Sill from San Rafael Swell	4.49±0.08	somewhat disturbed age spectrum
PR-15	hornblende	Monzonite porphyry	23.97±0.14	well-behaved
JN22703-1	biotite	Traverse Mountain volcanic	31.68±0.24	somewhat disturbed age spectrum
PR-9	sanidine	Painted Rocks welded tuff	34.00±0.13	one xenocryst
L33103-9	biotite	Traverse Mountain volcanic	35.25±0.13	well-behaved age spectrum

$^{40}Ar/^{39}Ar$ Analytical Methods and Results

Sanidine was separated from PR-9, hornblende from PR-15, groundmass concentrate from VY111902-7 and ZP 1501 and biotite from samples JN22703-1, L33103-9, MW1 and HM1. Samples were crushed and cleaned with either dilute Hydrofluoric or Hydrochloric acid and distilled water. The analyzed phases were separated with standard heavy liquid, magnetic separator and handpicking techniques. The mineral separates were then loaded into aluminum discs and irradiated for either 1

hour (NM-161) or 7 hours (NM-163 and NM-166) at the Nuclear Science Center in College Station, Texas.

Sixteen crystals of PR-9 sanidine were analyzed by the single-crystal laser fusion method. The age data are displayed on probability distribution diagrams (Deino and Potts, 1992). The seven other samples in this project were analyzed by the furnace incremental heating age spectrum method. Abbreviated analytical methods for the dated samples are given in Table 2, and details of the overall operation of the New Mexico Geochronology Research Laboratory are provided in the Appendix. The argon isotopic results are summarized in Tables 1 and 2 and listed in Tables 3 and 4.

Fifteen of the analyzed PR-9 sanidine crystals yield a near Gaussian population (Figure 1). A crystal with an apparent age 3-4 Ma years older than the other crystals was eliminated as a probable xenocryst before the calculation of the weighted mean age (34.00±0.11 Ma).

Biotite from samples MW1 yielded a fairly well-behaved age spectrum (Figure 2a). 99.3% of the ^{39}Ar released from MW1 is used to calculate a weighted mean age of 4.35±0.04 Ma. The radiogenic yields and K/Ca values are oscillatory. Steps D-L are evaluated with the inverse isochron technique and the ^{40}Ar/^{36}Ar intercept (291±14) is found to agree within error to the atmospheric value of 295.5 (Figure 2b).

The other three samples analyzed by biotite, HM1, L33103-9 and JN22703-1, yield slightly disturbed age spectra (Figures 3a-5a). A weighted mean age of 4.49±0.08 Ma is calculated from 98.8% of the ^{39}Ar released from HM1. The radiogenic yields and K/Ca values reveal the same correlated, oscillatory behavior seen in the MW1 age spectrum. Inverse isochron analysis of steps C-L reveals a ^{40}Ar/^{36}Ar intercept of 293±12 (Figure 3b) that agrees within error to the atmospheric value. L33103-9 and JN22703-1 yield increasing apparent ages, radiogenic yields and K/Ca values over the first ~10% of the ^{39}Ar released. Weighted mean ages have been calculated for these samples (L33103-9, 35.28±0.17 Ma and JN22703-1, 31.68±0.24 Ma) from the remaining portions of the age spectra. Both are slightly disturbed over portions of the age spectra with the disturbed portions correlating to changes in K/Ca value. Inverse isochron analysis of

steps D-L from both JN22703-1 and L33103-9 reveal $^{40}Ar/^{36}Ar$ intercepts that agree within error to the atmospheric value (Figures 4b and 5b).

Hornblende from PR-15 yields a fairly well-behaved age spectrum (Figure 6a). A weighted mean age of 23.97±0.14 Ma is calculated from 92.5% of the age spectrum. The first and last ~5% of ^{39}Ar reveal old apparent ages and relatively lower K/Ca values and radiogenic yields. As with all samples in this project, inverse isochron analysis (steps A-L, Figure 6b) reveals a $^{40}Ar/^{36}Ar$ intercept (302±15) that agrees within error to the atmospheric value.

VY111902-7 yields a well-behaved age spectrum (Figure 7a). A weighted mean age of 0.69±0.04 Ma is calculated from 100% of the ^{39}Ar released. Radiogenic yields decrease in the early and late heating steps. Steps A-I are evaluated with the inverse isochron technique and found to have a $^{40}Ar/^{36}Ar$ intercept that agrees within error to the atmospheric value (Figure 7b).

ZP 1501 groundmass concentrate reveals a somewhat disturbed age spectrum (Figure 8a). K/Ca values decrease over the entire age spectrum while radiogenic yields and apparent ages decrease over the first ~87%, followed by a rise in apparent age and radiogenic yield. Inverse isochron analysis of steps A-I yields a $^{40}Ar/^{36}Ar$ intercept within error of the atmospheric value (Figure 8b). The uniformly low radiogenic yields result in a clustering of data points near the $^{36}Ar/^{40}Ar$ axis which in turn results in a very large error on the inverse isochron analysis (0.10±0.29 Ma).

Discussion

With the exception of ZP 1501, the samples in this project provide reliable, precise information about the eruption ages of the volcanics (PR-9, L33103-9, JN22703-1, PR-15, and VY111902-7) and the intrusion age for the sill from the San Rafael Swell (HM1 and MW1). Although the ages assigned to HM1 and MW1 do not quite overlap at the 2 sigma level (MW1, 4.35±0.04 Ma and HM1, 4.49±0.08 Ma), the degassing behavior, K/Ca values and radiogenic yields are similar enough to suggest that they represent the same sill. The higher precision of MW1 suggests that the biotite from it was of higher

quality. If these two samples do represent the same sill, it is suggested that the age assigned to MW1 (4.35±0.04 Ma) is the more accurate age for the intrusion of the sill from the San Rafael Swell. The increasing radiogenic yields, K/Ca values and apparent ages revealed in the early portions of the L33103-9 and JN22703-1 age spectra, as well as the slightly disturbed later portions of the age spectra suggest slight alteration of the biotite samples. The alteration does not look severe enough, as suggested by the agreement of the integrated ages and the weighted mean ages, to significantly affect the weighted mean age of the samples. The old apparent ages in the low temperature steps of PR-15 and the higher temperature steps of PR-15, VY111902-7 and ZP 1501 that are correlated with a drop in K/Ca value, are suggestive of excess Ar ($^{40}Ar/^{36}Ar > 295.5$) in inclusions in the hornblende and phenocrysts in the groundmass concentrate. The combination of the young age and low K-content of ZP 1501 (~0.78% K2O verses 1.9% for VY111902-7) results in a very low precision date (80% error).

References Cited

Deino, A., and Potts, R., 1990. Single-Crystal $^{40}Ar/^{39}Ar$ dating of the Olorgesailie Formation, Southern Kenya Rift, J. Geophys. Res., 95, 8453-8470.

Deino, A., and Potts, R., 1992. Age-probability spectra from examination of single-crystal $^{40}Ar/^{39}Ar$ dating results: Examples from Olorgesailie, Southern Kenya Rift, Quat. International, 13/14, 47-53.

Mahon, K.I., 1996. The New "York" regression: Application of an improved statistical method to geochemistry, International Geology Review, 38, 293-303.

Samson, S.D., and, Alexander, E.C., Jr., 1987. Calibration of the interlaboratory $^{40}Ar/^{39}Ar$ dating standard, Mmhb-1, Chem. Geol., 66, 27-34.

Steiger, R.H., and Jäger, E., 1977. Subcommission on geochronology: Convention on the use of decay constants in geo- and cosmochronology. Earth and Planet. Sci. Lett., 36, 359-362.

Taylor, J.R., 1982. An Introduction to Error Analysis: The Study of Uncertainties in Physical Measurements, Univ. Sci. Books, Mill Valley, Calif., 270 p.

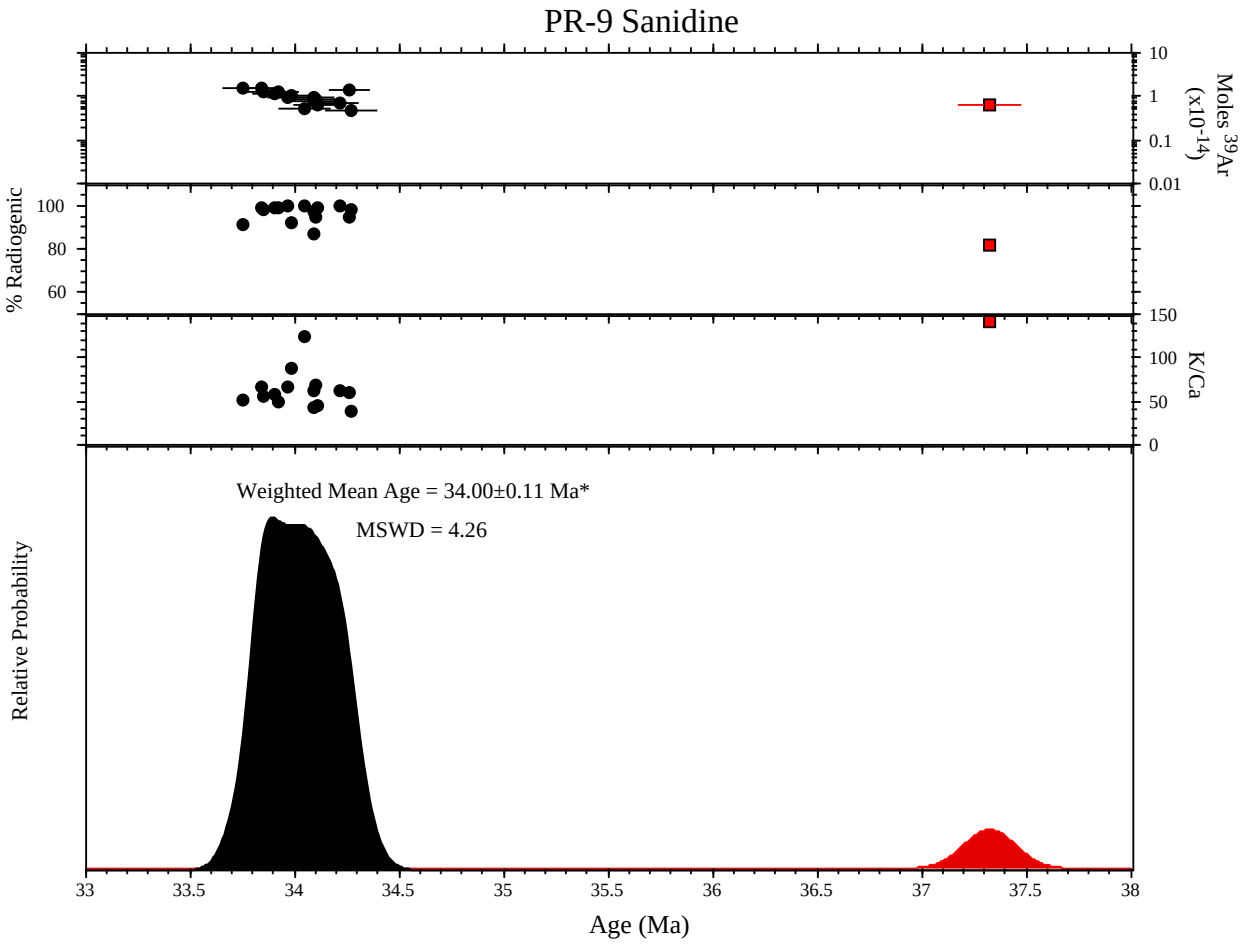

Figure 1. Age probability distribution diagram of PR-9 single crystal sanidine. Crystal shown in red was eliminated before calculation of weighted mean age. *2 sigma

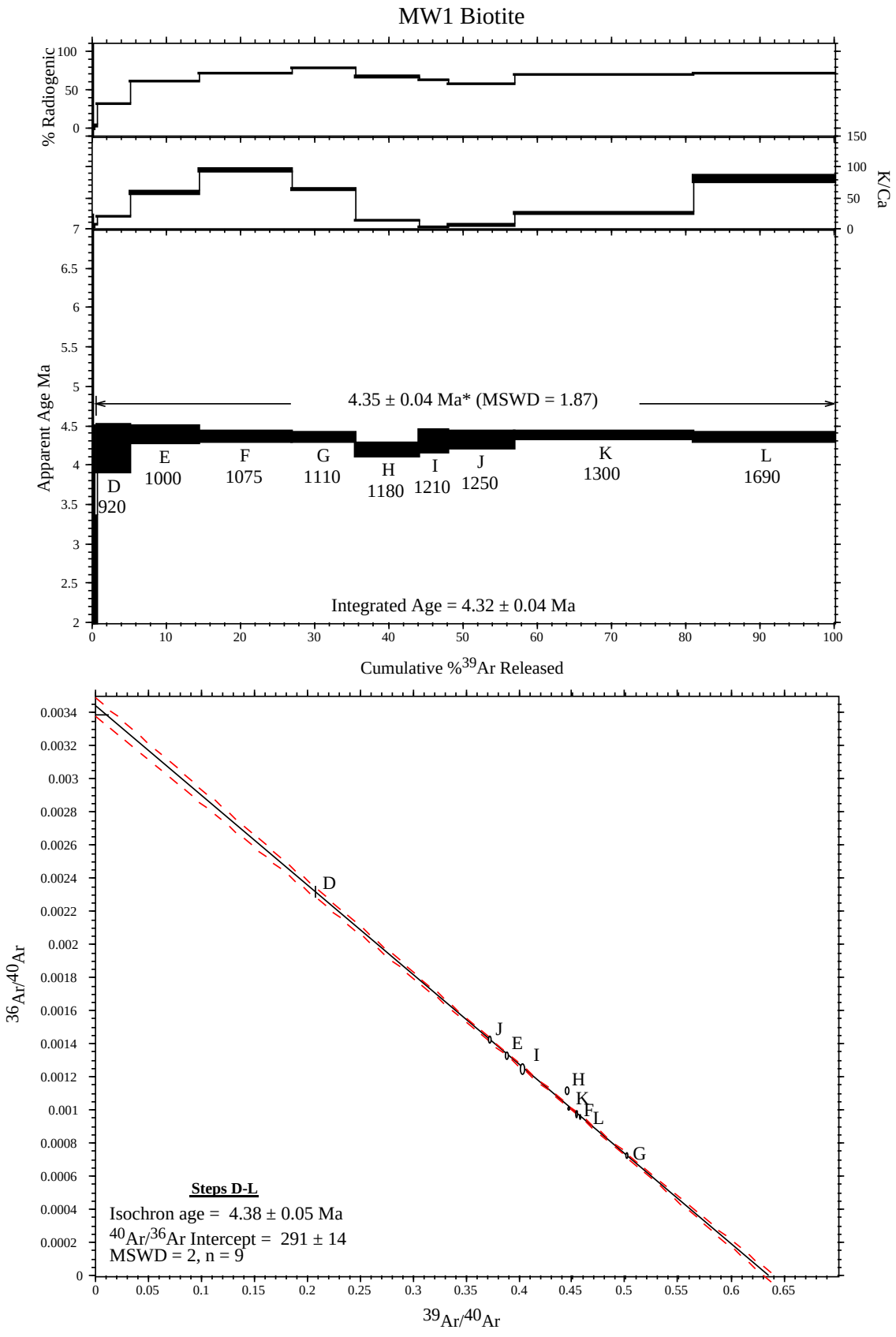

Figure 2. Age spectrum (a) and isochron (b) for sample MW1 biotite. *2sigma

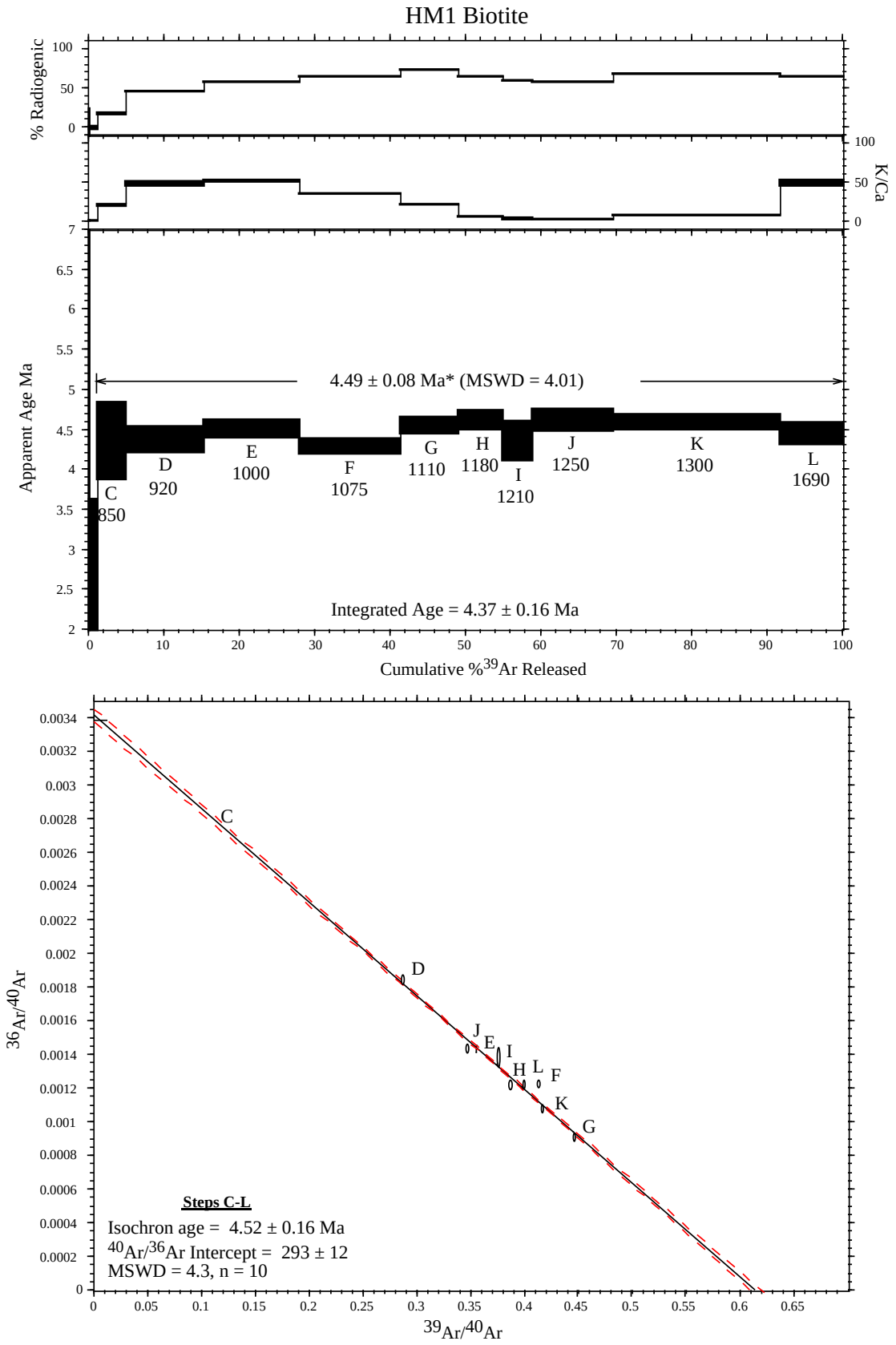

Figure 3. Age spectrum (a) and isochron (b) for sample HM1 biotite. *2sigma

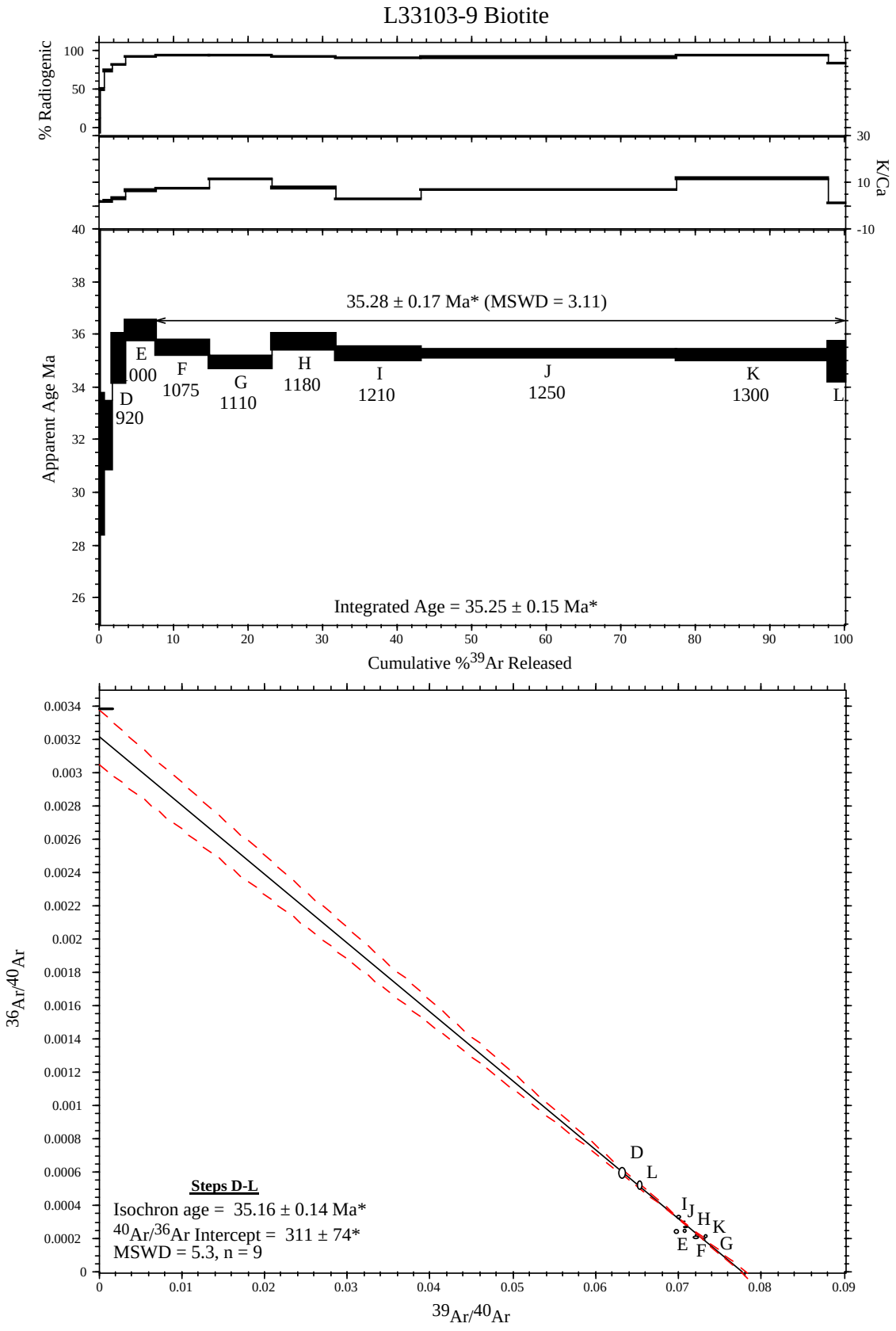

Figure 4. Age spectrum (a) and isochron (b) for sample HM1 biotite. *2sigma

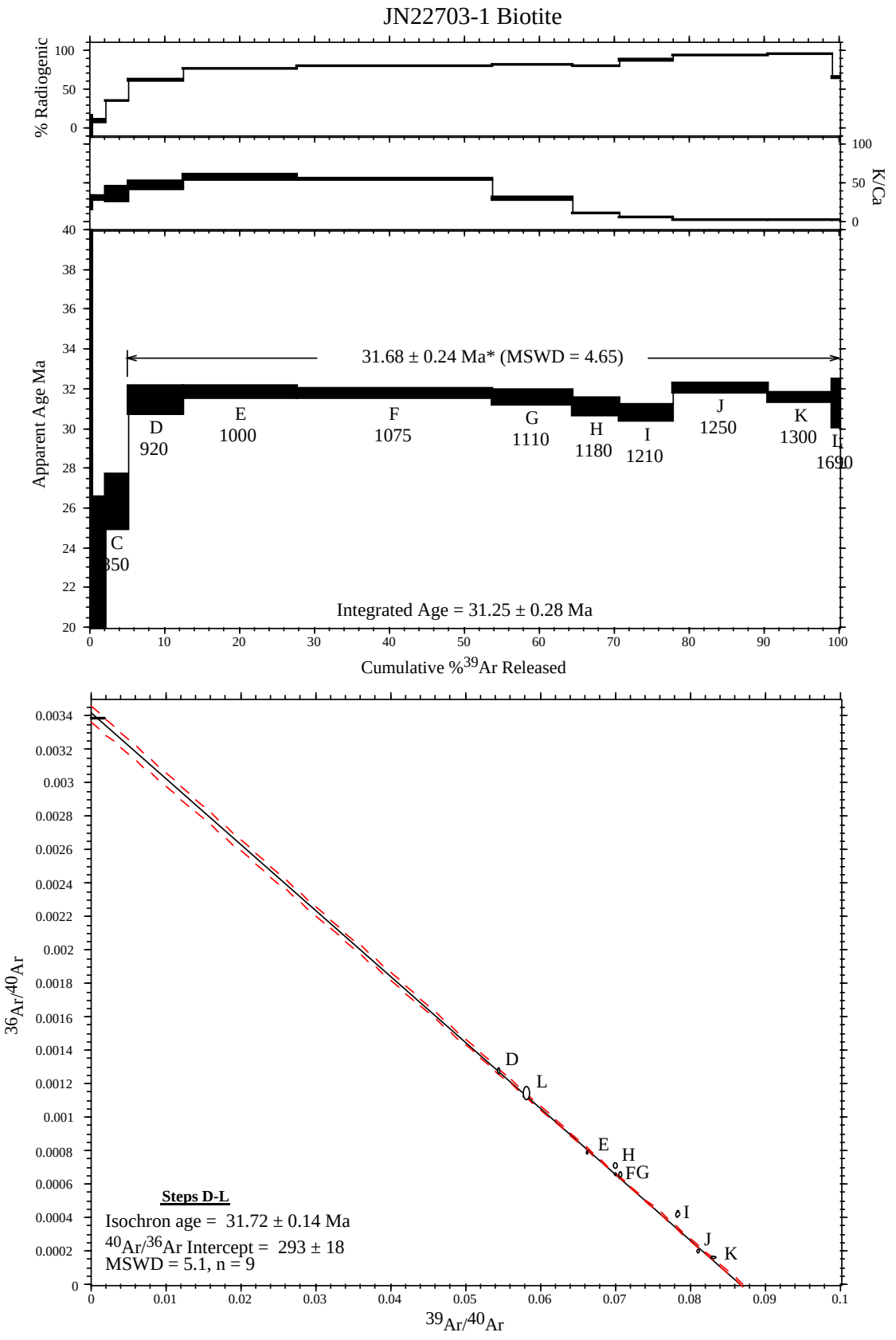

Figure 5. Age spectrum (a) and isochron (b) for sample JN22703-1 biotite. *2sigma

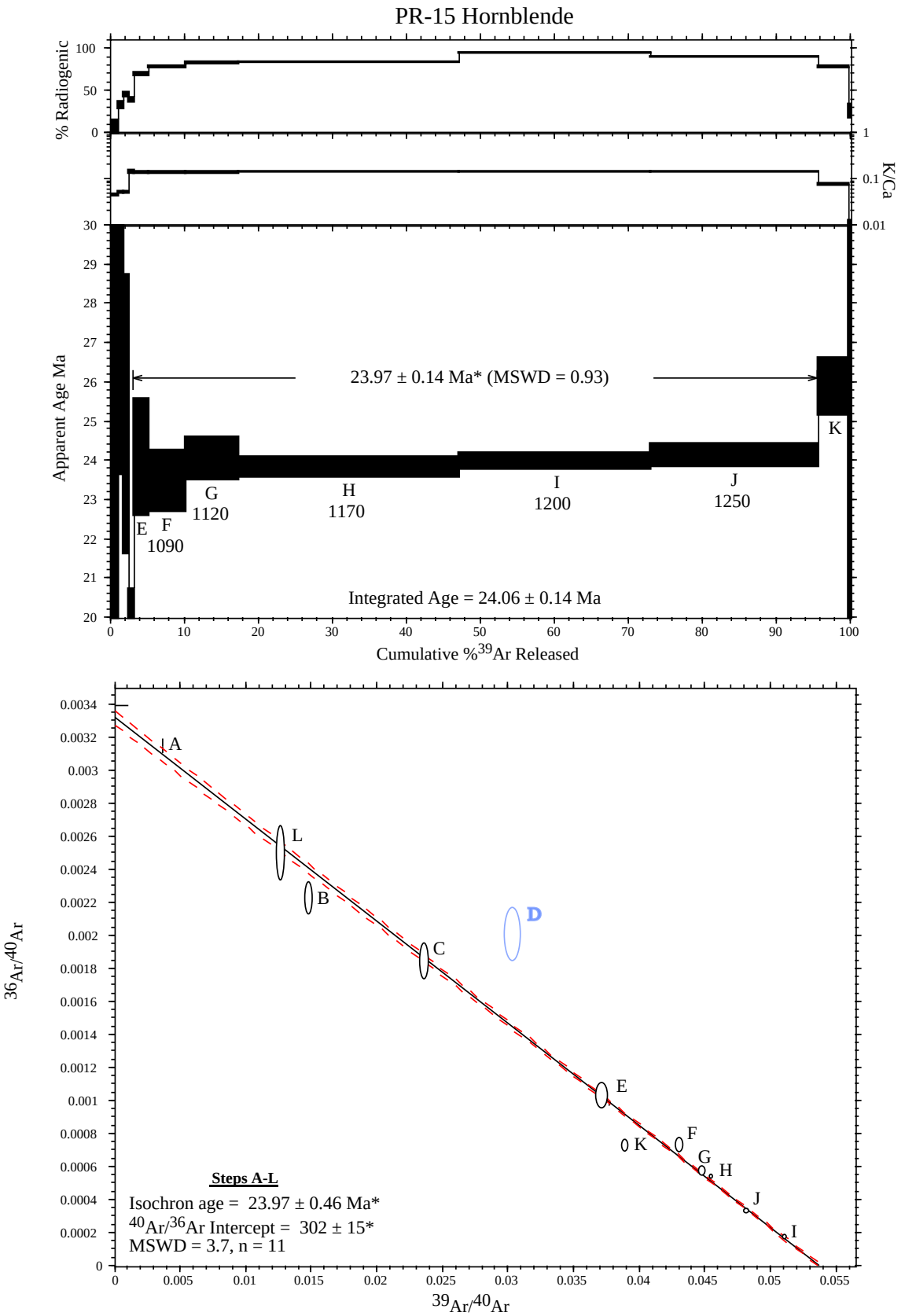

Figure 6. Age spectrum (a) and isochron (b) for sample PR-15 hornblende. Point shown in blue not included in isochron. *2sigma

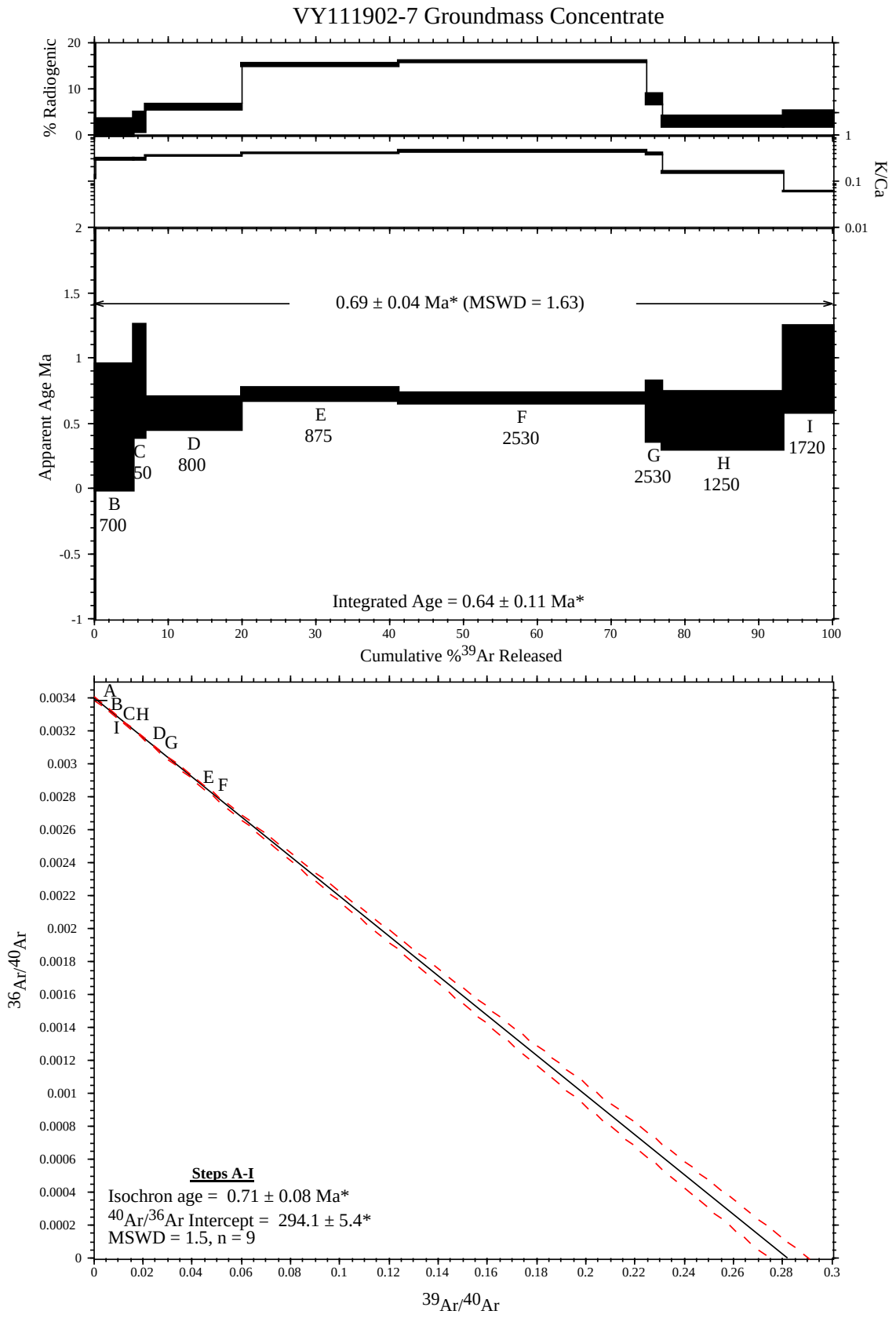

Figure 7. Age spectrum (a) and isochron (b) for sample VY111902-7 groundmass concentrate. *2 sigma

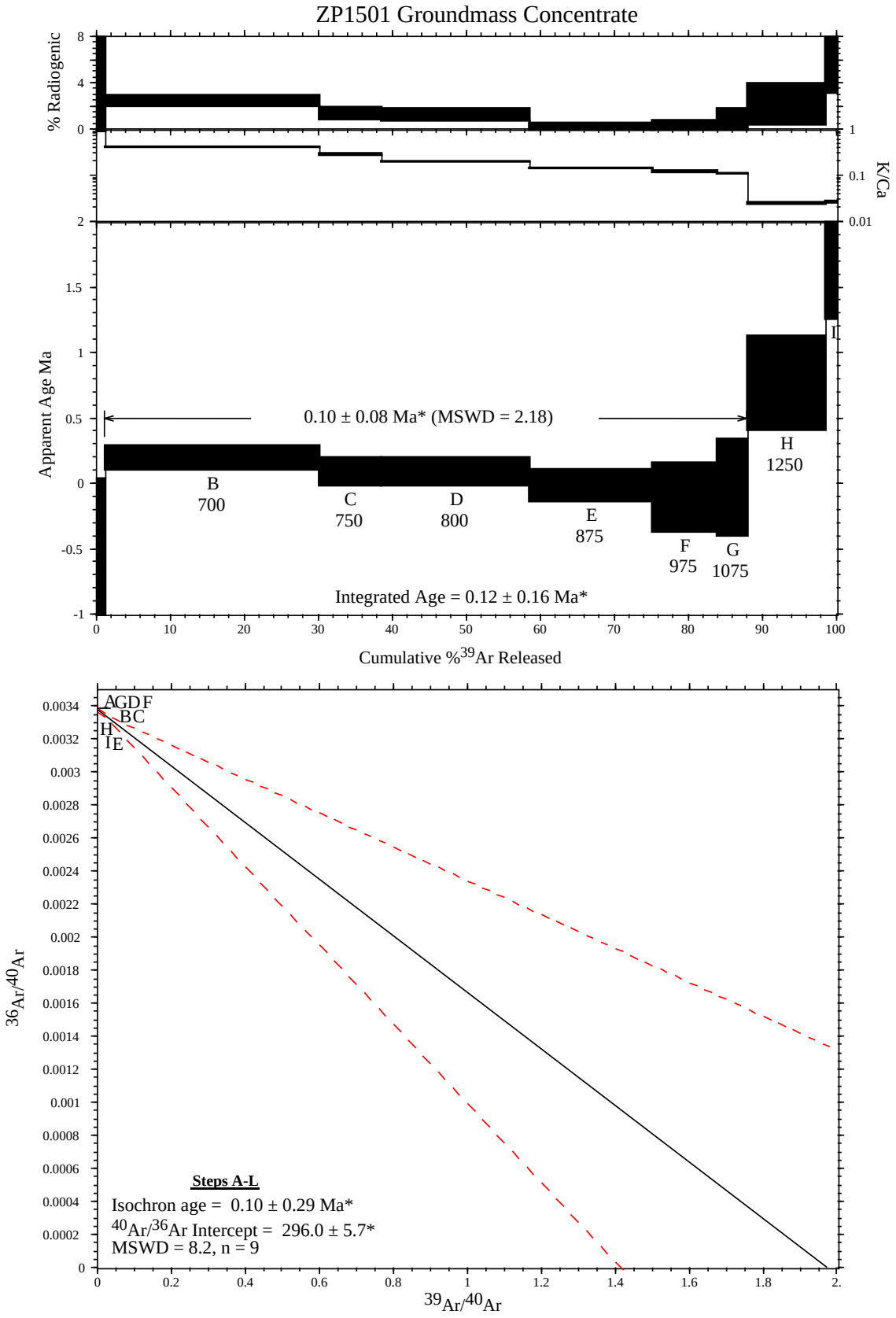

Figure 8. Age spectrum (a) and isochron (b) for sample ZP1501 groundmass concentrate. *2 sigma

Table 2. Summary of $^{40}Ar/^{39}Ar$ results and analytical methods

Sample	Location	Lab #	Irradiation	mineral	age analysis	# of crystals/steps	Age	±2σ	comments
ZP 1501	Crater Hill	53947	NM-163	¡roundmass concentrat	furnace step-heat	6	0.10	0.08	poor precision
VY111902	Veyo	53948	NM-163	¡roundmass concentrat	furnace step-heat	9	0.69	0.04	well-behaved age spectrum
MW1	San Rafael Swell	54100	NM-166	biotite	furnace step-heat	9	4.35	0.04	well-behaved age spectrum
HM1	San Rafael Swell	54101	NM-166	biotite	furnace step-heat	10	4.49	0.08	somewhat disturbed age spectrum
PR-15	-	53830	NM-161	hornblende	furnace step-heat	6	23.97	0.14	well-behaved age spectrum
JN22703-1	Traverse Mountain	54102	NM-166	biotite	furnace step-heat	9	31.68	0.24	somewhat disturbed age spectrum
PR-9	Painted Rocks	53844	NM-161	sanidine	laser total fusion	15	34.00	0.11	one xenocryst
L33103-9	Traverse Mountain	54114	NM-166	biotite	furnace step-heat	4	35.25	0.13	well-behaved age spectrum

Sample preparation and irradiation:

Mineral separates were prepared using standard crushing, dilute acid treatment, heavy liquid and hand-picking techniques.

Separates were loaded into a machined Al disc and irradiated for 1 hour (NM-163), 7 hours (NM-161) or 14 hours (NM-166) in the D-3 position, Nuclear Science Center, College Station, Neutron flux monitor Fish Canyon Tuff sanidine (FC-1). Assigned age = 27.84 Ma (Deino and Potts, 1990) relative to Mmhb-1 at 520.4 Ma (Samson and Alexander, 1987).

Instrumentation:

Mass Analyzer Products 215-50 mass spectrometer on line with automated all-metal extraction system.

Single crystal sanidine were fused by a 50 watt Synrad CO_2 laser.

Reactive gases removed during a 2 minute reaction with 2 SAES GP-50 getters, 1 operated at ~450°C and 1 at 20°C. Gas also exposed to a W filament operated at ~2000°C and a cold finger operated at -140°C.

Biotite, hornblende and groundmass concentrates were step-heated using a Mo double-vacuum resistance furnace. Heating duration in the furnace was 8 minutes for biotite, 9 minutes for groundmass concentrate and 10 minutes for hornblende. Reactive gases removed during furnace analysis by reaction with 3 SAES GP-50 getters, 2 operated at ~450°C and 1 at 20°C. Gas also exposed to a W filiment operated at ~2000°C.

Analytical parameters:

Electron multiplier sensitivity averaged 2.49 x 10^{-16} moles/pA for furnace NM-161samples, 1.53 x 10-16 moles/pA for laser NM-161 samples, 2.62 x 10^{-16} moles/pA for furnace NM-163 samples and 2.64 x 10-16 moles/pA for NM-166.

Total system blank and background averaged 724, 6.2, 2.1, 5.5, 4.5 x 10^{-18} moles at masses 40, 39, 38, 37 and 36, respectivelyfor the laser analyses. and 1400, 3.0, 1.0, 6.6, 5.6 x 10^{-18} moles at masses 40, 39, 38, 37 and 36, respectivelyfor the furnace analyses.

J-factors determined to a precision of ± 0.1% by CO_2 laser-fusion of 4 single crystals from each of 4 or 6 radial positions around the irradiation tray.

Correction factors for interfering nuclear reactions were determined using K-glass and CaF_2 and are as follows:

$(^{40}Ar/^{39}Ar)_K = 0.00020\pm0.0003$; $(^{36}Ar/^{37}Ar)_{Ca} = 0.00028\pm0.000005$; and $(^{39}Ar/^{37}Ar)_{Ca} = 0.0007\pm0.00002$.

Table 3. $^{40}Ar/^{39}Ar$ analytical data.

ID	$^{40}Ar/^{39}Ar$	$^{37}Ar/^{39}Ar$	$^{36}Ar/^{39}Ar$ (x 10^{-3})	$^{39}Ar_K$ (x 10^{-15} mol)	K/Ca	$^{40}Ar^*$ (%)	Age (Ma)	±1σ (Ma)
PR-9 sa, D15:161, single crystal sanidine, J=0.0006968±0.11%, D=1.00484±0.00092, NM-161, Lab#=53844								
06	29.67	0.0098	8.692	23.019	52.2	91.3	33.750	0.079
10	27.50	0.0078	1.111	23.401	65.6	98.8	33.837	0.058
11	27.78	0.0093	2.037	18.596	55.1	97.8	33.845	0.064
07	27.47	0.0087	0.8565	17.752	58.4	99.1	33.899	0.085
01	27.64	0.0103	1.359	17.982	49.4	98.6	33.919	0.076
04	27.39	0.0077	0.3811	13.741	66.2	99.6	33.962	0.075
16	29.57	0.0059	7.707	15.058	86.8	92.3	33.982	0.099
12	27.49	0.0041	0.5055	7.824	124.5	99.5	34.04	0.11
08	31.52	0.0121	14.03	11.540	42.3	86.9	34.086	0.097
03	28.28	0.0082	3.069	13.738	62.6	96.8	34.089	0.080
15	28.84	0.0076	4.958	12.671	67.5	94.9	34.094	0.094
02	27.79	0.0112	1.347	9.464	45.6	98.6	34.112	0.094
09	27.51	0.0081	0.1205	10.236	63.2	99.9	34.214	0.066
13	29.11	0.0084	5.409	20.144	61.0	94.5	34.255	0.079
05	28.07	0.0132	1.853	6.841	38.7	98.1	34.270	0.100
14	36.76	0.0036	22.87	9.517	141.2	81.6	37.32	0.13
Mean age ± 2σ	n=16		MSWD=49.70		67.5 ±56.3		34.09	0.30

Notes:

Isotopic ratios corrected for blank, radioactive decay, and mass discrimination, not corrected for interferring reactions.

Ages calculated relative to FC-1 Fish Canyon Tuff sanidine interlaboratory standard at 27.84 Ma.

Errors quoted for individual analyses include analytical error only, without interferring reaction or J uncertainties.

Mean age is weighted mean age of Taylor (1982). Mean age error is weighted error
of the mean (Samson and Alexander, 1987), and also
incorporates uncertainty in J factors and irradiation correction uncertainties.

Decay constants and isotopic abundances after Steiger and Jaeger (1977).

symbol preceding sample ID denotes analyses excluded from mean age calculations.

Discrimination = 1.00484 ± 0.00092

Correction factors:

$(^{39}Ar/^{37}Ar)_{Ca}$ = 0.0007 ± 2e-05

$(^{36}Ar/^{37}Ar)_{Ca}$ = 0.00028 ± 5e-06

$(^{38}Ar/^{39}Ar)_{K}$ = 0.01077

$(^{40}Ar/^{39}Ar)_{K}$ = 0.0002 ± 0.0003

Table 4. $^{40}Ar/^{39}Ar$ analytical data.

	ID	Power (Watts)	$^{40}Ar/^{39}Ar$	$^{37}Ar/^{39}Ar$	$^{36}Ar/^{39}Ar$ (x 10^{-3})	$^{39}Ar_K$ (x 10^{-15} mol)	K/Ca	$^{40}Ar^*$ (%)	^{39}Ar (%)	Age (Ma)	±1σ (Ma)
	ZP 1501 gm, B1:163, groundmass concentrate, 193.92, J=0.0001116, D=1.00623, NM-163, Lab#=53947-01										
†	A	575	2914.7	0.5507	9953.1	0.477	0.93	-0.9	1.2	-5.32	2.68
	B	650	39.20	1.242	129.7	11.9	0.41	2.5	30.1	0.20	0.05
	C	700	31.56	1.795	105.8	3.45	0.28	1.4	38.4	0.09	0.05
	D	750	37.50	2.544	126.1	8.3	0.20	1.2	58.5	0.09	0.05
	E	825	55.38	3.479	188.7	6.86	0.15	-0.1	75.1	-0.02	0.06
	F	925	88.78	4.208	303.4	3.61	0.12	-0.6	83.8	-0.11	0.13
	G	1025	117.4	4.688	399.0	1.75	0.11	-0.1	88.0	-0.03	0.19
†	H	1200	171.2	20.17	572.3	4.29	0.025	2.2	98.4	0.77	0.18
†	I	1670	146.3	19.26	468.5	0.653	0.026	6.5	100.0	1.94	0.34
	Integrated age ± 2σ			n=9		41.3		K2O=0.98 %		0.12	0.16
	Plateau ± 2σ steps B-G			n=6	MSWD=2.18	35.9	0.26		86.9	0.10	0.08
	VY111902-7 gm, B2:163, groundmass concentrate, 197.42, J=0.0001116, D=1.00623, NM-163, Lab#=53948-01										
	A	575	9822.4	3.999	33474.2	0.121	0.13	-0.7	0.1	-13.96	9.62
	B	650	221.0	1.701	740.6	4.23	0.30	1.1	4.1	0.47	0.24
	C	700	138.5	1.668	455.2	1.20	0.31	3.0	5.2	0.82	0.22
	D	750	46.41	1.386	147.7	10.6	0.37	6.2	15.8	0.58	0.06
	E	825	23.44	1.223	67.53	17.4	0.42	15.3	34.6	0.72	0.03
	F	925	21.37	1.130	61.03	27.4	0.45	16.0	69.2	0.69	0.02
	G	1025	37.91	1.312	118.7	1.65	0.39	7.7	71.5	0.59	0.11
	H	1200	86.52	3.203	285.0	13.4	0.16	3.0	91.3	0.52	0.11
	I	1670	129.5	8.197	425.3	5.45	0.062	3.5	100.0	0.91	0.17
	Integrated age ± 2σ			n=9		81.5		K2O=1.88 %		0.64	0.11
	Plateau ± 2σ steps A-I			n=9	MSWD=1.63	81.5	0.35		100.0	0.69	0.04
	PR-15 hb, B6:161, 10.57 mg hornblende, J=0.0007187, D=1.0065, NM-161, Lab#=53830-01										
†	A	750	271.9	11.47	858.1	0.236	0.044	7.1	0.7	25.0	4.9
†	B	850	67.25	10.07	155.4	0.178	0.051	32.9	1.2	28.7	2.5
†	C	950	42.41	10.12	80.66	0.207	0.050	45.8	1.8	25.2	1.8
†	D	980	33.03	3.538	68.90	0.152	0.14	39.3	2.2	16.8	2.0
	E	1010	26.68	3.714	28.19	0.499	0.14	69.9	3.7	24.09	0.74
	F	1040	23.20	3.667	18.02	1.27	0.14	78.4	7.5	23.47	0.39
	G	1070	22.33	3.727	13.57	1.80	0.14	83.4	13.0	24.06	0.28
	H	1120	21.96	3.533	12.86	7.5	0.14	84.0	38.9	23.83	0.12
	I	1150	19.52	3.574	4.173	6.47	0.14	95.2	65.7	24.00	0.10
	J	1200	20.75	3.608	7.946	5.68	0.14	90.1	93.9	24.14	0.14
†	K	1250	25.58	6.573	20.62	1.04	0.078	78.3	99.6	25.90	0.36
†	L	1650	76.66	42.95	202.8	0.079	0.012	26.5	100.0	26.9	5.0
	Integrated age ± 2σ			n=12		25.1		K2O=1.27 %		24.06	0.23
	Plateau ± 2σ steps E-J			n=6	MSWD=0.93	23.2	0.14		92.5	23.97	0.14
	MW1 bi, E14:166, Biotite, 10.17 mg, J=0.0015424, D=1.00484, NM-166, Lab#=54100-01										
†	A	600	4586.1	0.0764	15408.7	0.006	6.7	0.7	0.0	89.27	199.88
†	B	700	32.34	0.1710	108.0	0.681	3.0	1.4	0.3	1.27	1.61
†	C	800	14.30	0.0727	46.62	1.10	7.0	3.7	0.7	1.48	0.94
	D	870	4.809	0.0254	11.15	11.5	20.1	31.5	5.1	4.21	0.15
	E	950	2.583	0.0087	3.405	24.0	58.8	61.1	14.4	4.38	0.05
	F	1025	2.202	0.0053	2.144	32.6	95.9	71.2	26.9	4.36	0.03
	G	1060	1.993	0.0079	1.443	22.4	64.4	78.6	35.5	4.36	0.03
	H	1130	2.248	0.0364	2.510	22.1	14.0	67.2	44.1	4.20	0.05
	I	1160	2.476	0.1347	3.176	10.2	3.8	62.5	48.0	4.30	0.07
	J	1200	2.681	0.0803	3.829	23.1	6.4	58.0	56.9	4.33	0.05
	K	1250	2.239	0.0198	2.247	62.7	25.7	70.4	81.0	4.38	0.02
	L	1640	2.195	0.0063	2.129	49.3	81.3	71.4	100.0	4.35	0.03
	Integrated age ± 2σ			n=12		259.7		K2O=6.36 %		4.32	0.04
	Plateau ± 2σ steps D-L			n=9	MSWD=1.87	257.9	47.8		99.3	4.35	0.04
	HM1 bi, E15:166, Biotite, 8.24 mg, J=0.0015409, D=1.00484, NM-166, Lab#=54101-01										
†	A	600	2281.0	0.4989	7769.3	0.291	1.0	-0.6	0.1	-41.49	34.62
†	B	700	121.1	0.5447	410.5	2.18	0.94	-0.1	1.2	-0.46	2.04
	C	800	8.983	0.0242	25.09	7.38	21.1	17.5	5.0	4.36	0.24
	D	870	3.470	0.0105	6.414	20.5	48.6	45.4	15.3	4.38	0.08
	E	950	2.815	0.0099	4.034	24.8	51.4	57.7	27.9	4.51	0.05
	F	1025	2.421	0.0143	2.961	26.6	35.7	63.9	41.3	4.29	0.05

	ID	Power (Watts)	$^{40}Ar/^{39}Ar$	$^{37}Ar/^{39}Ar$	$^{36}Ar/^{39}Ar$ (x 10^{-3})	$^{39}Ar_K$ (x 10^{-15} mol)	K/Ca	$^{40}Ar^*$ (%)	^{39}Ar (%)	Age (Ma)	±1σ (Ma)
	Integrated age ± 2σ		n=12			197.7		K2O=5.98 %		4.37	0.16
	Plateau ± 2σ	steps C-L	n=10	MSWD=4.01		195.3	25.7		98.8	4.49	0.08
	JN22703-1 bi, E16:166, Biotite, 2.90 mg, J=0.0015395, D=1.00484, NM-166, Lab#=54102-01										
†	A	600	1099.0	0.0200	3712.5	0.253	25.6	0.2	0.3	5.38	22.71
†	B	700	86.05	0.0162	263.1	1.45	31.6	9.6	2.0	22.90	1.83
†	C	800	26.88	0.0141	58.63	2.54	36.1	35.6	5.1	26.35	0.69
	D	870	18.36	0.0106	23.46	6.21	48.0	62.2	12.5	31.46	0.34
	E	950	15.09	0.0088	11.92	12.6	57.9	76.7	27.6	31.86	0.15
	F	1025	14.31	0.0092	9.360	21.8	55.2	80.7	53.6	31.77	0.11
	G	1060	14.16	0.0168	9.108	9.1	30.4	81.0	64.5	31.57	0.18
	H	1130	14.24	0.0447	9.962	5.20	11.4	79.4	70.7	31.12	0.23
	I	1160	12.77	0.0763	5.397	5.86	6.7	87.6	77.7	30.81	0.21
	J	1200	12.37	0.1908	2.516	10.7	2.7	94.1	90.4	32.04	0.12
	K	1250	12.03	0.2331	1.973	7.19	2.2	95.3	99.0	31.57	0.12
	L	1640	17.25	0.1831	19.99	0.81	2.8	65.8	100.0	31.28	0.60
	Integrated age ± 2σ		n=12			83.7		K2O=7.20 %		31.25	0.28
	Plateau ± 2σ	steps D-L	n=9	MSWD=4.65		79.4	33.4		94.9	31.68	0.24
	L33103-9 bi, H1:166, Biotite, 2.46 mg, J=0.0015295, D=1.00484, NM-166, Lab#=54114-02										
†	A	600	339.1	0.2962	1116.1	0.109	1.7	2.7	0.1	25.51	11.45
†	B	700	22.71	0.2792	38.47	0.421	1.8	50.0	0.7	31.10	1.34
†	C	800	15.96	0.2539	14.29	0.76	2.0	73.7	1.6	32.17	0.63
†	D	870	15.74	0.1701	9.840	1.43	3.0	81.6	3.5	35.10	0.48
†	E	950	14.31	0.0781	3.652	3.27	6.5	92.5	7.6	36.17	0.20
†	F	1025	13.87	0.0695	2.991	5.52	7.3	93.7	14.6	35.49	0.15
†	G	1060	13.63	0.0443	2.863	6.72	11.5	93.8	23.2	34.94	0.12
†	H	1130	14.15	0.0657	3.678	6.63	7.8	92.4	31.6	35.71	0.15
	I	1160	14.30	0.1897	4.766	9.0	2.7	90.3	43.1	35.27	0.12
	J	1200	14.17	0.0726	4.288	27.0	7.0	91.1	77.4	35.27	0.08
	K	1250	13.70	0.0435	2.733	16.0	11.7	94.1	97.7	35.24	0.10
	L	1640	15.29	0.4441	8.556	1.81	1.1	83.7	100.0	34.98	0.39
	Integrated age ± 2σ		n=12			78.6		K2O=8.02 %		35.25	0.15
	Plateau ± 2σ	steps I-L	n=4	MSWD=0.19		53.7	7.5		68.4	35.25	0.13

Notes:

Isotopic ratios corrected for blank, radioactive decay, and mass discrimination, not corrected for interferring reactions.
Ages calculated relative to FC-1 Fish Canyon Tuff sanidine interlaboratory standard at 27.84 Ma.
Errors quoted for individual analyses include analytical error only, without interferring reaction or J uncertainties.
Integrated age calculated by recombining isotopic measurements of all steps.
Integrated age error calculated by recombining errors of isotopic measurements of all steps.
Plateau age is inverse-variance-weighted mean of selected steps.
Plateau age error is inverse-variance-weighted mean error (Taylor, 1982) times root MSWD where MSWD>1.
Plateau and integrated ages incorporate uncertainties in interferring reaction corrections and J factors.
Decay constants and isotopic abundances after Steiger and Jaeger (1977).
# symbol preceding sample ID denotes analyses excluded from plateau age calculations.
Discrimination = 1.0065 ± 0.0015
Correction factors:
$(^{39}Ar/^{37}Ar)_{Ca}$ = 0.0007 ± 2e-05
$(^{36}Ar/^{37}Ar)_{Ca}$ = 0.00028 ± 5e-06
$(^{38}Ar/^{39}Ar)_{K}$ = 0.01077
$(^{40}Ar/^{39}Ar)_{K}$ = 0.0002 ± 0.0003

APPENDIX

New Mexico Bureau of Mines and Mineral Resources

Procedures of the New Mexico Geochronology Research Laboratory

For the Period June 1998 – present

Matthew Heizler
William C. McIntosh
Richard Esser
Lisa Peters

$^{40}Ar/^{39}Ar$ and K-Ar dating

Often, large bulk samples (either minerals or whole rocks) are required for K-Ar dating and even small amounts of xenocrystic, authigenic, or other non-ideal behavior can lead to inaccuracy. The K-Ar technique is susceptible to sample inhomogeneity as separate aliquots are required for the potassium and argon determinations. The need to determine absolute quantities (i.e. moles of $^{40}Ar^*$ and ^{40}K) limits the precision of the K-Ar method to approximately 1% and also, the technique provides limited potential to evaluate underlying assumptions. In the $^{40}Ar/^{39}Ar$ variant of the K-Ar technique, a sample is irradiated with fast neutrons thereby converting ^{39}K to ^{39}Ar through a (n,p) reaction. Following irradiation, the sample is either fused or incrementally heated and the gas analyzed in the same manner as in the conventional K-Ar procedure, with one exception, no argon spike need be added.

Some of the advantages of the $^{40}Ar/^{39}Ar$ method over the conventional K-Ar technique are:

1. A single analysis is conducted on one aliquot of sample thereby reducing the sample size and eliminating sample inhomogeneity.
2. Analytical error incurred in determining absolute abundances is reduced by measuring only isotopic ratios. This also eliminates the need to know the exact weight of the sample.
3. The addition of an argon spike is not necessary.
4. The sample does not need to be completely fused, but rather can be incrementally heated. The $^{40}Ar/^{39}Ar$ ratio (age) can be measured for each fraction of argon released and this allows for the generation of an age spectrum.

The age of a sample as determined with the $^{40}Ar/^{39}Ar$ method requires comparison of the measured $^{40}Ar/^{39}Ar$ ratio with that of a standard of known age. Also, several isotopes of other elements (Ca, K, Cl, Ar) produce argon during the irradiation procedure and must be corrected for. Far more in-depth details of the determination of an apparent age via the $^{40}Ar/^{39}Ar$ method are given in Dalrymple et al. (1981) and McDougall and Harrison (1988).

Analytical techniques

Sample Preparation and irradiation details

Mineral separates are obtained in various fashions depending upon the mineral of interest, rock type and grain size. In almost all cases the sample is crushed in a jaw crusher and ground in a disc grinder and then sized. The size fraction used generally corresponds to the largest size possible which will permit obtaining a pure mineral separate. Following sizing, the sample is washed and dried. For plutonic and metamorphic rocks and lavas, crystals are separated using standard heavy liquid, Franz magnetic and hand-picking techniques. For volcanic sanidine and plagioclase, the sized sample is reacted with 15% HF acid to remove glass and/or matrix and then thoroughly washed prior to heavy liquid and magnetic separation. For groundmass concentrates, rock fragments are selected which do not contain any visible phenocrysts.

The NMGRL uses either the Ford reactor at the University of Michigan or the Nuclear Science Center reactor at Texas A&M University. At the Ford reactor, the L67 position is used (unless otherwise noted) and the D-3 position is always used at the Texas A&M reactor. All of the Michigan irradiations are carried out underwater without any shielding for thermal neutrons, whereas the Texas irradiations are in a dry location, which is shielded with B and Cd. Depending upon the reactor used, the mineral separates are loaded into either holes drilled into Al discs or into 6 mm I.D. quartz tubes. Various Al discs are used. For Michigan, either six hole or twelve hole, 1 cm diameter discs are used and all holes are of equal size. Samples are placed in the 0, 120 and 240° locations and standards in the 60, 180 and 300° locations for the six-hole disc. For the twelve-hole disc, samples are located at 30, 60, 120, 150, 210, 240, 300, and 330° and standards at 0, 90, 180 and 270 degrees. If samples are loaded into the quartz tubes, they are wrapped in Cu foil with standards interleaved at ~0.5 cm intervals. For Texas, 2.4 cm diameter discs contain either sixteen or six sample holes with smaller holes used to hold the standards. For the six-hole disc, sample locations are 30, 90, 150, 210, 270 and 330° and standards are at 0, 60, 120, 180, 240 and 300°. Samples are located at 18, 36, 54, 72, 108, 126, 144, 162, 198, 216, 234, 252, 288, 306, 324, 342 degrees and standards at 0, 90, 180 and 270 degrees in the sixteen hole disc. Following sample loading into the discs, the discs are stacked, screwed together and sealed

in vacuo in either quartz (Michigan) or Pyrex (Texas) tubes.

Extraction Line and Mass Spectrometer details

The NMGRL argon extraction line has both a double vacuum Mo resistance furnace and a CO_2 laser to heat samples. The Mo furnace crucible is heated with a W heating element and the temperature is monitored with a W-Re thermocouple placed in a hole drilled into the bottom of the crucible. A one inch long Mo liner is placed in the bottom of the crucible to collect the melted samples. The furnace temperature is calibrated by either/or melting Cu foil or with an additional thermocouple inserted in the top of the furnace down to the liner. The CO_2 laser is a Synrad 10W laser equipped with a He-Ne pointing laser. The laser chamber is constructed from a 3 3/8" stainless steel conflat and the window material is ZnS. The extraction line is a two stage design. The first stage is equipped with a SAES GP-50 getter, whereas the second stage houses two SAES GP-50 getters and a tungsten filament. The first stage getter is operated at 450°C as is one of the second stage getters. The other second stage getter is operated at room temperature and the tungsten filament is operated at ~2000°C. Gases evolved from samples heated in the furnace are reacted with the first stage getter during heating. Following heating, the gas is expanded into the second stage for two minutes and then isolated from the first stage. During second stage cleaning, the first stage and furnace are pumped out. After gettering in the second stage, the gas is expanded into the mass spectrometer. Gases evolved from samples heated in the laser are expanded through a cold finger operated at -140°C and directly into the second stage. Following cleanup, the gas in the second stage and laser chamber is expanded into the mass spectrometer for analysis.

The NMGRL employs a MAP-215-50 mass spectrometer, which is operated in static mode. The mass spectrometer is operated with a resolution ranging between 450 to 600 at mass 40 and isotopes are detected on a Johnston electron multiplier operated at ~2.1 kV with an overall gain of about 10,000 over the Faraday collector. Final isotopic intensities are determined by linear regression to time zero of the peak height versus time following gas introduction for each mass. Each mass intensity is corrected for mass spectrometer baseline and background and the extraction system blank.

Blanks for the furnace are generally determined at the beginning of a run while the furnace is cold and then between heating steps while the furnace is cooling. Typically, a blank is

run every three to six heating steps. Periodic furnace hot blank analysis reveals that the cold blank is equivalent to the hot blank for temperatures less than about 1300°C. Laser system blanks are generally determined between every four analyses. Mass discrimination is measured using atmospheric argon which has been dried using a Ti-sublimation pump. Typically, 10 to 15 replicate air analyses are measured to determine a mean mass discrimination value. Air pipette analyses are generally conducted 2-3 times per month, but more often when samples sensitive to the mass discrimination value are analyzed. Correction factors for interfering nuclear reactions on K and Ca are determined using K-glass and CaF_2, respectively. Typically, 3-5 individual pieces of the salt or glass are fused with the CO_2 laser and the correction factors are calculated from the weighted mean of the individual determinations.

Data acquisition, presentation and age calculation

Samples are either step-heated or fused in a single increment (total fusion). Bulk samples are often step-heated and the data are generally displayed on an age spectrum or isochron diagram. Single crystals are often analyzed by the total fusion method and the results are typically displayed on probability distribution diagrams or isochron diagrams.

The Age Spectrum Diagram

Age spectra plot apparent age of each incrementally heated gas fraction versus the cumulative % $^{39}Ar_K$ released, with steps increasing in temperature from left to right. Each apparent age is calculated assuming that the trapped argon (argon not produced by *in situ* decay of ^{40}K) has the modern day atmospheric $^{40}Ar/^{36}Ar$ value of 295.5. Additional parameters for each heating step are often plotted versus the cumulative $\%^{39}Ar_K$ released. These auxiliary parameters can aid age spectra interpretation and may include radiogenic yield (percent of ^{40}Ar which is not atmospheric), K/Ca (determined from measured Ca-derived ^{37}Ar and K-derived ^{39}Ar) and/or K/Cl (determined from measured Cl-derived ^{38}Ar and K-derived ^{39}Ar). Incremental heating analysis is often effective at revealing complex argon systematics related to excess argon, alteration, contamination, ^{39}Ar recoil, argon loss, etc. Often low-temperature heating steps have low radiogenic yields and apparent ages with relatively high errors due mainly to

loosely held, non-radiogenic argon residing on grain surfaces or along grain boundaries. An entirely or partially flat spectrum, in which apparent ages are the same within analytical error, may indicate that the sample is homogeneous with respect to K and Ar and has had a simple thermal and geological history. A drawback to the age spectrum technique is encountered when hydrous minerals such as micas and amphiboles are analyzed. These minerals are not stable in the ultra-high vacuum extraction system and thus step-heating can homogenize important details of the true ^{40}Ar distribution. In other words, a flat age spectrum may result even if a hydrous sample has a complex argon distribution.

The Isochron Diagram

Argon data can be plotted on isotope correlation diagrams to help assess the isotopic composition of Ar trapped at the time of argon closure, thereby testing the assumption that trapped argon isotopes have the composition of modern atmosphere which is implicit in age spectra. To construct an "inverse isochron" the $^{36}Ar/^{40}Ar$ ratio is plotted versus the $^{39}Ar/^{40}Ar$ ratio. A best fit line can be calculated for the data array which yields the value for the trapped argon (Y-axis intercept) and the $^{40}Ar^*/^{39}Ar_K$ value (age) from the X-axis intercept. Isochron analysis is most useful for step-heated or total fusion data, which have a significant spread in radiogenic yield. For young or low K samples, the calculated apparent age can be very sensitive to the composition of the trapped argon and therefore isochron analysis should be preformed routinely on these samples (cf. Heizler and Harrison, 1988). For very old (>Mesozoic) samples or relatively old sanidines (>mid-Cenozoic) the data are often highly radiogenic and cluster near the X-axis thereby making isochron analysis of little value.

The Probability Distribution Diagram

The probability distribution diagram, which is sometimes referred to as an ideogram, is a plot of apparent age versus the summation of the normal distribution of each individual analysis (Deino and Potts, 1992). This diagram is most effective at displaying single crystal laser fusion data to assess the distribution of the population. The K/Ca, radiogenic yield, and the moles of ^{39}Ar for each analysis are also often displayed for each sample as this allows for visual ease in identifying apparent age correlations between, for instance, plagioclase contamination, signal size and/or radiogenic concentrations. The error (1σ) for each age analysis is generally shown by the horizontal lines in the moles of ^{39}Ar section. Solid symbols represent the analyses used for the weighted mean age calculation and the generation of the solid line on the ideogram, whereas open symbols represent data omitted from the age calculation. If shown, a dashed line represents the probability distribution of all of the displayed data. The diagram is most effective for displaying the form of the age distribution (i.e. gaussian, skewed, etc.) and for identifying xenocrystic or other grains, which fall outside of the main population.

Error Calculations

For step-heated samples, a plateau for the age spectrum is defined by the steps indicated. The plateau age is calculated by weighting each step on the plateau by the inverse of the variance and the error is calculated by either the method of Samson and Alexander (1987) or Taylor (1982). A mean sum weighted deviates (MSWD) value is determined by dividing the Chi-squared value by n-1 degrees of freedom for the plateau ages. If the MSWD value is outside the 95% confidence window (cf. Mahon, 1996; Table 1), the plateau or preferred age error is multiplied by the square root of the MSWD.

For single crystal fusion data, a weighted mean is calculated using the inverse of the variance to weight each age determination (Taylor, 1982). Errors are calculated as described for the plateau ages above.

Isochron ages, $^{40}Ar/^{36}Ar_i$ values and MSWD values are calculated from the regression results obtained by the York (1969) method.

References cited

Dalrymple, G.B., Alexander, E.C., Jr., Lanphere, M.A., and Kraker, G.P., 1981. Irradiation of samples for $^{40}Ar/^{39}Ar$ dating using the Geological Survey TRIGA reactor. U.S.G.S., Prof. Paper, 1176.

Deino, A., and Potts, R., 1990. Single-Crystal $^{40}Ar/^{39}Ar$ dating of the Olorgesailie Formation, Southern Kenya Rift, J. Geophys. Res., 95, 8453-8470.

Deino, A., and Potts, R., 1992. Age-probability spectra from examination of single-crystal $^{40}Ar/^{39}Ar$ dating results: Examples from Olorgesailie, Southern Kenya Rift, Quat. International, 13/14, 47-53.

Fleck, R.J., Sutter, J.F., and Elliot, D.H., 1977. Interpretation of discordant $^{40}Ar/^{39}Ar$ age-spectra of Mesozoic tholieiites from Antarctica, Geochim. Cosmochim. Acta, 41, 15-32.

Heizler, M. T., and Harrison, T. M., 1988. Multiple trapped argon components revealed by $^{40}Ar/^{39}Ar$ analysis, Geochim. Cosmochim. Acta, 52, 295-1303.

Mahon, K.I., 1996. The New "York" regression: Application of an improved statistical method to geochemistry, International Geology Review, 38, 293-303.

McDougall, I., and Harrison, T.M., 1988. Geochronology and thermochronology by the ^{40}Ar-^{39}Ar method. Oxford University Press.

Samson, S.D., and, Alexander, E.C., Jr., 1987. Calibration of the interlaboratory $^{40}Ar/^{39}Ar$ dating standard, Mmhb-1, Chem. Geol., 66, 27-34.

Steiger, R.H., and Jäger, E., 1977. Subcommission on geochronology: Convention on the use of decay constants in geo- and cosmochronology. Earth and Planet. Sci. Lett., 36, 359-362.

Taylor, J.R., 1982. An Introduction to Error Analysis: The Study of Uncertainties in Physical Measurements, Univ. Sci. Books, Mill Valley, Calif., 270 p.

York, D., 1969. Least squares fitting of a straight line with correlated errors, Earth and Planet. Sci. Lett., 5, 320-324.